AUT Journal of Mechanical Engineering

AUT J. Mech. Eng., 7(3) (2023) 283-296
DOI: 10.22060/ajme.2024.22545.6067

Enhancing Mechanical Properties of Ultrasonically-Treated 3D-Printed Acrylonitrile-Butadiene-Styrene and Polylactic Acid Parts: A Full Factorial Design Approach

Vahid Fartashvand[1], Abdolvahed Kami[2]*, Abbasali Bagheri[2]

[1] Department of Industrial Design, Faculty of Art, Alzahra University, Tehran, Iran
[2] Faculty of Mechanical Engineering, Semnan University, Semnan, Iran

ABSTRACT: This study explores the enhancement of mechanical properties in 3D-printed polylactic acid and acrylonitrile-butadiene-styrene parts through ultrasonic treatment. Tensile samples were fabricated using fused filament fabrication with varying infill percentages (60% and 100%) and layer thicknesses (0.15 mm and 0.30 mm). Post-processing involved a high-power ultrasonic treatment for 2 seconds, followed by tensile testing. The results demonstrated an average 10% increase in tensile strength for both acrylonitrile-butadiene-styrene and polylactic acid after ultrasonic treatment, with the highest tensile strengths measured at approximately 41 MPa and 38 MPa, respectively. However, strain at fracture experienced a decline, except in the samples with an infill percentage of 100 and a number of layers of 10. Scanning electron microscopy revealed dimensional changes and raster merging, more pronounced in 60% and 100% infill samples, respectively. The study employed a comprehensive full factorial design of experiments and finite element simulation for ultrasonic treatment setup design. The interaction of 3D printing and ultrasonic treatment parameters was investigated, with the infill percentage exhibiting the most substantial impact on the ultimate tensile strength. The results highlight the potential of ultrasonic treatment to enhance mechanical properties, reduce defects, and improve the structural integrity of 3D-printed components.

Review History:
Received: Jul. 09, 2023
Revised: Dec. 09, 2023
Accepted: Feb. 19, 2024
Available Online: Feb. 25, 2024

Keywords:
3D-printing
Additive manufacturing
Ultrasonic Treatment
ABS
PLA

1- Introduction

Fused filament fabrication (FFF) is a prevalent additive manufacturing technique, particularly in applications ranging from consumer products to industries such as the military, automotive, design offices, and medicine [1, 2]. Despite its widespread use, the mechanical properties of 3D-printed polymeric products, especially in comparison to injection-molded counterparts, often fall short due to layered structures, poor interlayer adhesion, and the presence of voids [3, 4]. However, the cost-effectiveness of this prototyping method is a solid motivation to improve their properties. Nevertheless, postprocessing treatments such as heat, ultrasonic, and hot pressing can improve the mechanical characteristics of 3D-printed components such that printed parts can be used as a final product [5, 6]. The use of ultrasonic treatment (UT) has demonstrated the potential to improve mechanical qualities and reduce 3D printing defects [7-9]. As shown in Fig. 1, the UT of 3D printing parts can be done either in situ or ex situ. In the in-situ treatment, the nozzle or the printing bed vibrates. In this case, no additional step is added to the 3D printing procedure; nevertheless, it does require more complex equipment. On the other hand, the ex-situ UTs utilize standard 3D printing equipment; however, it adds a postprocessing phase, which lengthens and complicates the entire production process.

Li et al. [6, 7, 10] used ultrasonic vibrations on ABS and PLA 3D-printed components. Consequently, the voids are decreased, the adhesion of the layers is improved, and the mechanical qualities of the 3D-printed objects are enhanced. Guivier, Kuebler, Swanson, Lawson, Fernandez-Ballester, Negahban, and Sealy [8] investigated the influence of interlayer ultrasonic treatment on the mechanical characteristics of 3D-printed ABS components. The ultrasonic vibration was applied in two configurations: four (L4) and eight (L8) layers of 3D printing. When ultrasonic peening was conducted at the L8 configuration, no substantial changes in the mechanical properties were found. At the L4 configuration, fracture strain (ductility) and elastic modulus are lowered, although tensile strength is enhanced. Tofangchi, Han, Izquierdo, Iyengar and Hsu [9] investigated the influence of ultrasonic vibrations on the interlayer adhesion of ABS. They applied transverse ultrasonic vibrations at a frequency of 34.4 kHz to the nozzle of an FFF printer. Compared to traditional FFF printing, the interlayer adhesion increased by approximately 10 percent. Maidin, Muhamad, and Pei [11] examined three alternative configurations of ultrasonic devices attached to a desktop FFF machine. They intended to investigate the viability of improving surface finish with ultrasonic vibrations. The three configurations involve attaching the ultrasonic transducer directly to the nozzle body, linking the transducer to the

*Corresponding author's email: akami@semnan.ac.ir

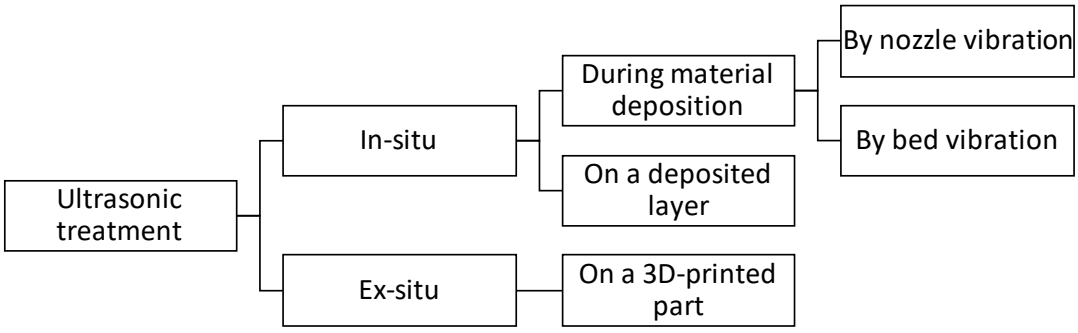

Fig. 1. Classification of UT configurations used for the treatment of parts produced by 3D-printing

Table 1. Physical and mechanical properties of ABS and PLA filaments [16]

Physical properties	ABS	PLA
Density (g/cm^3)	1.05	1.24
Melt Flow Rate (g/10min)	18.9	7
Mechanical properties		
Tensile strength (MPa)	47	60
Elongation at break (%)	37	6

nozzle via sheet metal, and clamping the workpiece to the ultrasonic transducer's surface. The results indicated that the 3D-printed parts with the second setup had the best surface finish. Polymer matrix composites have also been 3D printed employing ultrasonic vibrations. In this case, ultrasonic vibrations were used to improve the impregnation of the reinforcing fiber, which in turn improved the mechanical properties of the composites [12, 13].

The limited mechanical properties of 3D-printed polymeric products are mostly attributed to their layered structure, inadequate interlayer adhesion, and the presence of voids. While postprocessing treatments like heat, ultrasonic, and hot pressing have shown promise in enhancing mechanical characteristics, no prior research has comprehensively analyzed the interplay of 3D printing and ultrasonic parameters. This study aims to fill a gap in existing research by investigating how UT uniquely influences the mechanical properties of 3D-printed ABS and PLA parts. It specifically explores the combined impact of 3D printing and ultrasonic parameters.

2- Materials and Methods

2- 1- Tensile Sample 3D Printing

ABS and PLA were selected as target materials due to their widespread use in FFF 3D printing [14, 15]. The physical and mechanical properties of the ABS and PLA filaments (Guangzhou Yousu Plastic Technology Co., China) are summarized in Table 1. The effects of UT on the tensile characteristics of these materials were studied. The tensile samples were prepared following the ASTM E8M standard (see Fig. 2), with a thickness of 3 mm. Tensile tests were conducted using the Santam STM-150 universal testing machine, which has a capacity of 15 tons, at a speed of 5 mm/min.

Using an FFF desktop 3D printer (Sizan-3L 3D printer made by Sizan Pardazesh Kavir Co., Kashan, Iran), ABS and PLA tensile samples were 3D printed. Table 2 presents the factors related to 3D printing. The infill pattern is rectilinear with the raster angle of +45°/-45°, as illustrated in Fig. 3. Along with the infill percentage, the influence of the number of layers was studied; the samples were 3D printed with 10 and 20 layers.

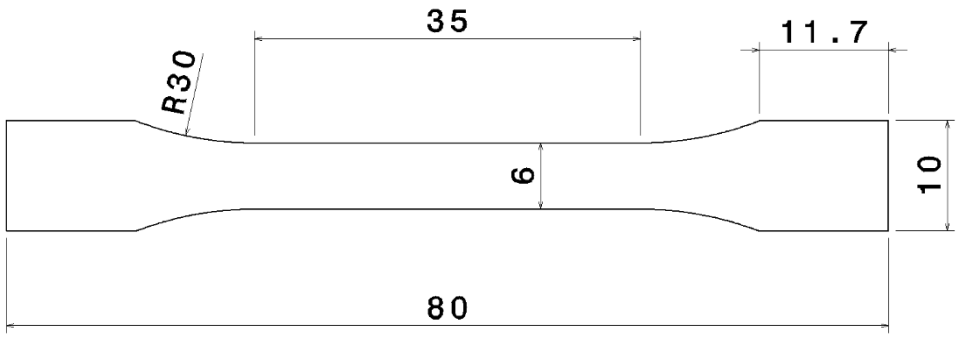

Fig. 2. Geometry of the tensile test samples (all values are in mm, and the sample's thickness is equal to 3 mm)

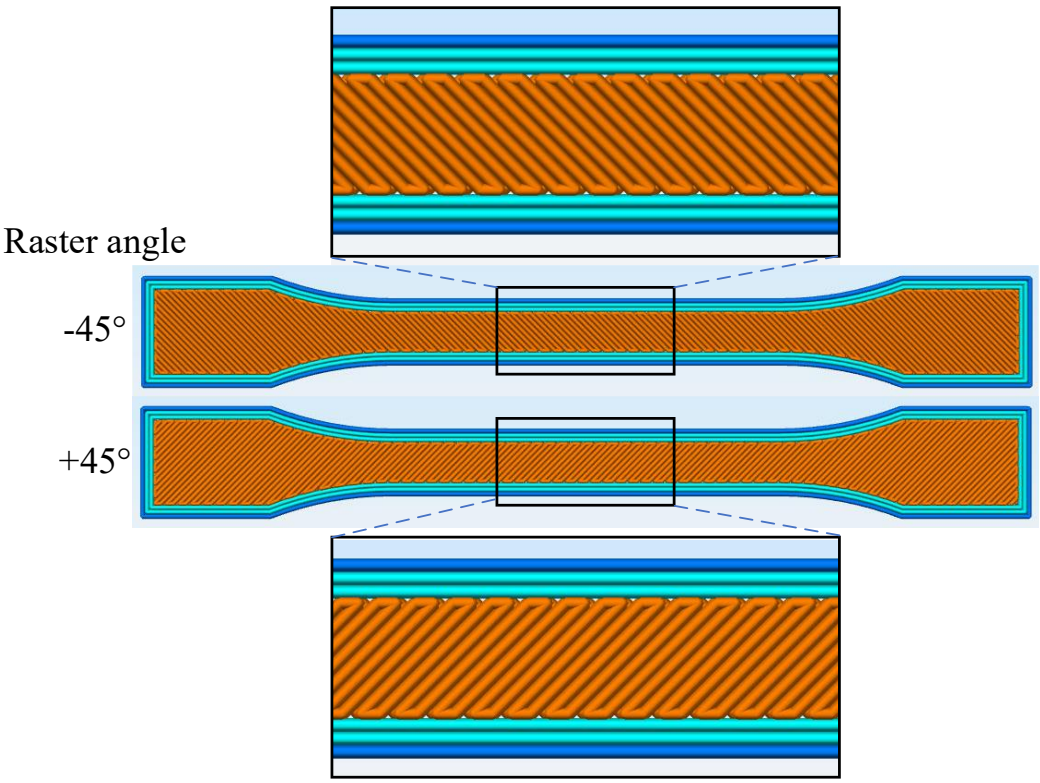

Fig. 3. Illustration of the raster orientations in subsequent layers of the 3D-printed tensile samples with a raster angle of +45°/-45°

2- 2- Ultrasonic Treatment Setup

Abaqus software was used to do a finite element simulation, from which the UT setup was designed. The ultrasonic apparatus consists of a nominal 2 kW ultrasonic transducer that transforms electrical energy to low-amplitude 20 kHz vibration. Then, an Al7075-T6 alloy booster modifies the vibration amplitude and delivers it to an acoustic horn (made of Al7075-T6 alloy). The horn transmits vibrations to printed components. The head of the horn is an anti-node plane with the maximum amplitude of vibration (see Fig. 4). The surface of the horn has dimensions of 20 × 110 mm, which are greater than the dimensions of the 3D-printed parts, and ensures that all sections of the tensile specimens have been ultrasonically treated. However, it was a one-sided treatment.

This ultrasonic stack was mounted on a plastic welding machine (made by Farasout Tajhiz Iranian Co., Tehran, Iran). A fixture was fabricated to secure the samples during UT and restrict their extra-dimensional changes. The fixture is clamped on the machine's table, and the samples are placed inside it (see Fig. 5).

Table 2. Main 3D printing parameters and their values

3D printing variables	Value
Nozzle diameter (mm)	0.5
Solid layers (top, bottom, shell)	2
Infill (%)	60, 100
Internal fill pattern	Rectilinear (+45°/-45°)
Perimeter 3D printing speed (mm/s)	50
Infill 3D printing speed (mm/s)	60
Nozzle temperature (°C)	ABS (250), PLA (210)
Bed temperature (°C)	ABS (70), PLA (50)

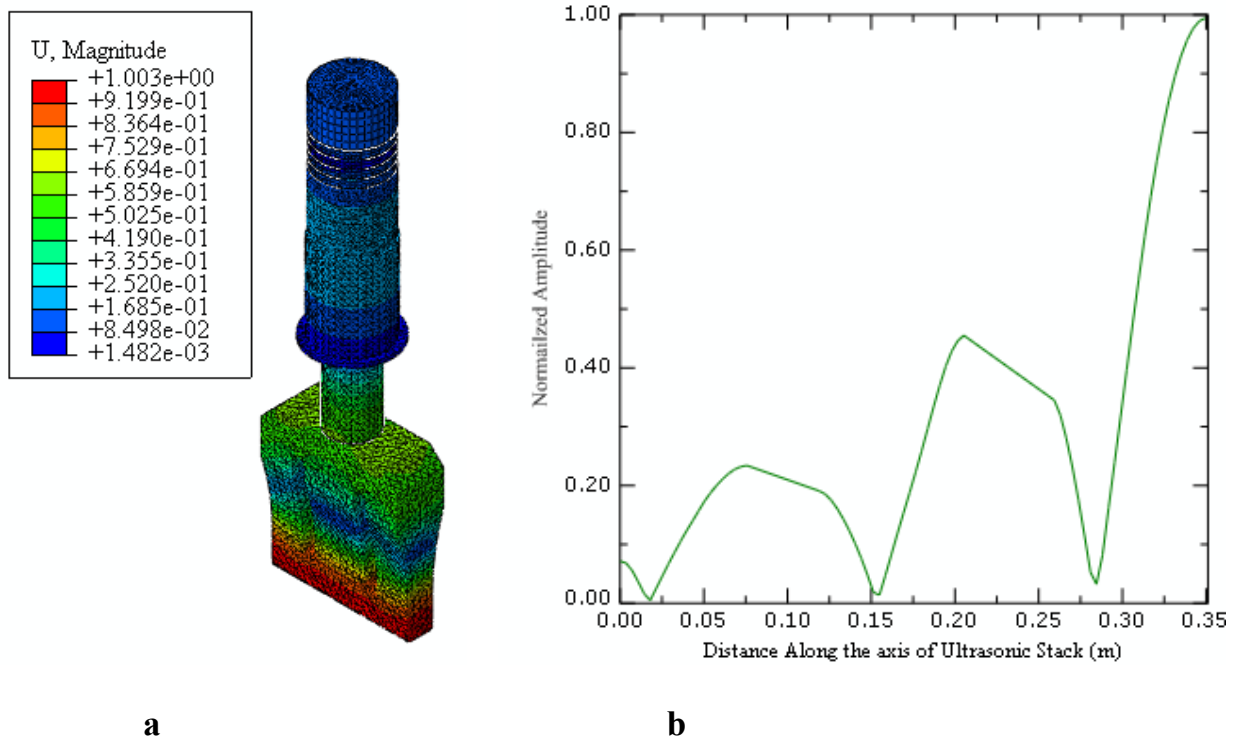

Fig. 4. a) FEM analysis of ultrasonic stack (frequency 20 kHz) and b) distribution of the normalized ultrasonic vibration amplitude along the axis of the ultrasonic stack

Fig. 5. The UT setup (the fixture is clamped on the ultrasonic welding machine table)

Table 3. UT parameters

Variable	Value
UT time (s)	2
Delay time (s)	0.5
Dwell time (s)	0.5
Ultrasonic power (kW)	2
Ultrasonic frequency (kHz)	20
UT pressure (kPa)	3.5

Table 3 presents the UT parameters and their corresponding values. Before ultrasonic vibrations are applied, samples are mechanically loaded. This step's duration is known as delay time, which does not affect the quality of the treatment. Then, the ultrasonic generator turns on automatically, and the vibrations are applied to the specimen. The time of applying ultrasonic vibration is UT time and is equal to 2 s. Then, the generator is switched off, and the mechanical load presses the specimen for a dwell time set to 0.5 s. This step helps build and strengthen links between the rasters of the 3D-printed part. The ultrasonic head is finally raised, and the sample is removed from the fixture. This time is selected according to some pretests to obtain valuable data for comparison of UT sample with non-treated one.

2- 3- Design of Experiments

The influence of both 3D printing and UT parameters was studied. These parameters include the infill percentage, the number of layers, and the treatment time. Each parameter has been evaluated at two levels. Thus, eight experiments were conducted for each of the ABS and PLA components using a full factorial design. Table 4 shows the list of these tests. The infill percentage was set to 60% and 100% to examine the potential dimension changes resulting from the UT. Moreover, layer interfaces of 3D-printed parts are a source of discontinuity. Hence, the number of layers may influence the transition of ultrasonic vibrations and, consequently, the quality of UT. To evaluate this hypothesis, the number of layers was chosen to be ten and twenty. Finally, the samples

Table 4. Two-level factorial design of tensile test samples of ABS and PLA

Sample No.	Infill (%)	Treatment time (s)	Number of layers	Tensile strength of PLA (MPa)	Tensile strength of ABS (MPa)
1	60	0	10	25.41±1.66	28.07±2.13
2	60	0	20	17.78±1.93	24.19±1.65
3	60	2	10	28.31±0.43	30.04±1.06
4	60	2	20	19.48±3.66	28.48±1.61
5	100	0	10	35.22±1.52	37.54±0.98
6	100	0	20	31.85±1.78	37.61±1.35
7	100	2	10	37.94±2.35	40.3±1.79
8	100	2	20	35.94±2.01	40.81±0.49

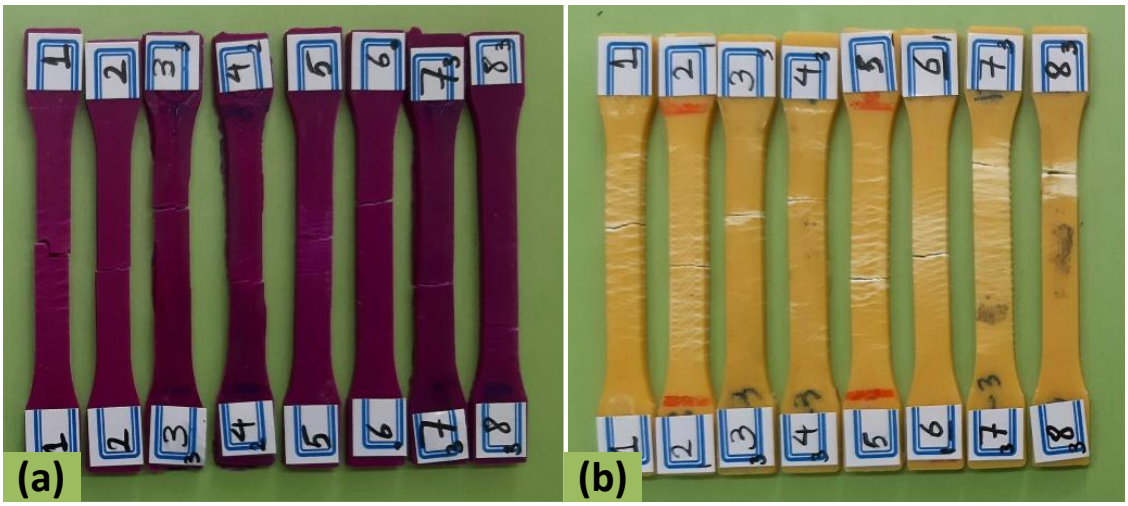

Fig. 6. The tensile samples after the test (a) PLA and (b) ABS

were subjected to ultrasonic vibrations for 2 seconds, and the findings were compared to those obtained without UT.

3- Results and Discussions

3- 1- Tensile Test Results

Fig. 6 depicts the samples after conducting tensile tests. Each test has been repeated three times, and the average of these tests is presented in this figure. As one may observe, the surface of the samples contains distinct lines, particularly in the ABS samples. This observation is due to the sliding of nearby rasters. Another fact is that the fracture section of the samples is nearly perpendicular to the direction of loading. This remark is comparable to the brittle fracture of metals. Thus, it can be argued that brittle fracture is the predominant fracture mode. A more detailed discussion on the examination of the fracture sections of ABS and PLA samples is given in the following section.

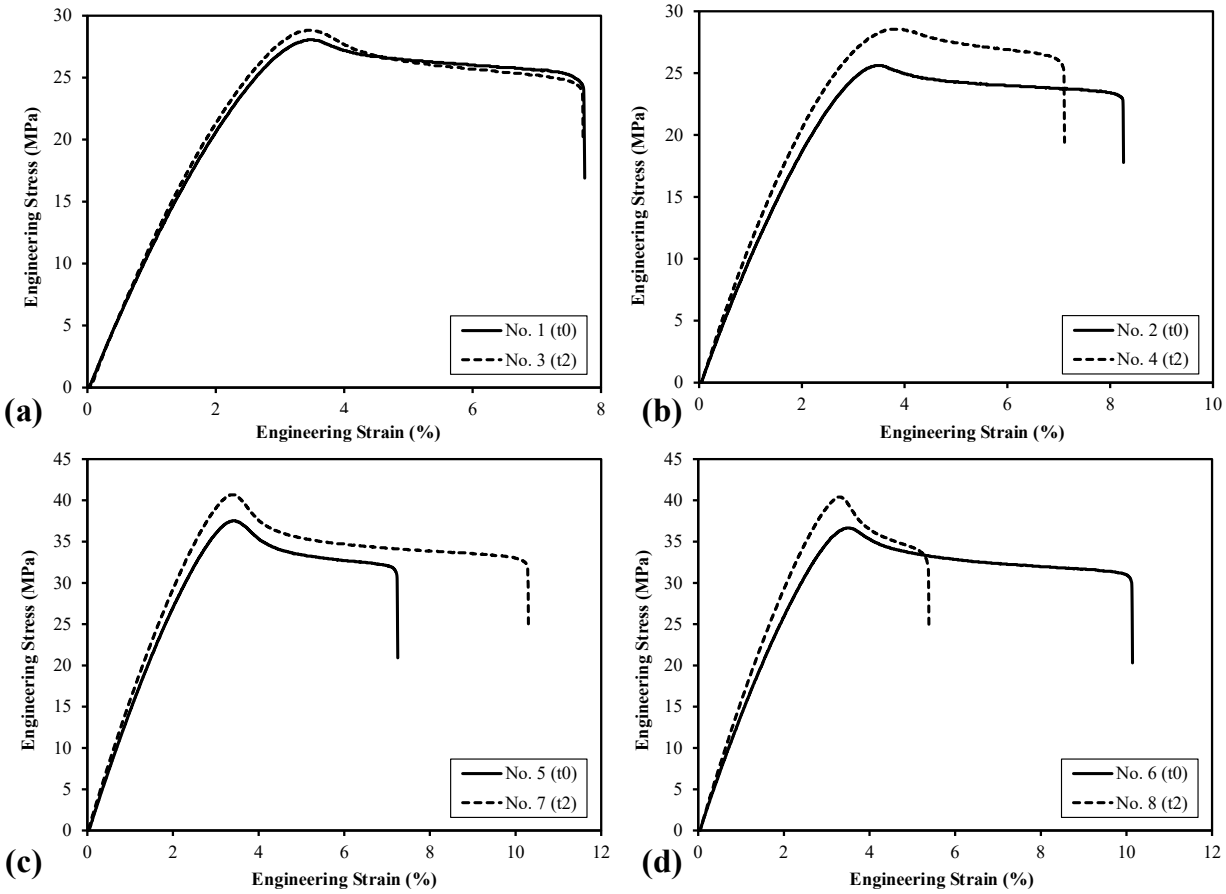

Fig. 7. Comparison of engineering stress-strain curves for ABS samples before and after UT; (a) 60% infill, 10 layers, (b) 60% infill, 20 layers, (c) 100% infill, 10 layers, (d) 100% infill, 20 layers

The engineering stress-strain curves of the ABS and PLA samples are illustrated in Figs. 7 and 8, respectively. The results depicted in these figures are comparable to the findings reported in [6, 10]. These figures show the effects of the number of layers and UT on the tensile behavior of the samples. According to Fig. 7, UT enhances the tensile strength of the ABS samples. However, the change in elongation is dependent on the number of layers. In other words, the formability of the ABS samples with a higher number of layers decreases after UT, which implies that they become more brittle. This behavior implies an interaction between the number of layers and UT. In PLA samples, regardless of the number of layers, the application of ultrasonic treatment increased strength and decreased elongation (see Fig. 8). The increase in the tensile strength could be related to the improvement of the bonding strength of layers and the decrease of porosities in the structure of the 3D-printed samples [13]. These phenomena can be attributed to several interrelated factors: First, UT induces localized heating in the interlayer regions of the 3D-printed samples [17, 18]. This thermal energy promotes partial melting of the polymer material, especially in regions with lower infill percentages. The melted material tends to flow and fuse, reducing the voids and porosities in the structure. Second, the application of ultrasonic vibrations, especially in samples with lower infill percentages, leads to compression effects. The pressure exerted by the ultrasonic horn compacts the material, reducing voids and empty spaces in the structure. However, the decrease in elongation due to UT is speculated to be due to the degradation of the polymeric molecules. Transfer of ultrasonic vibration in ABS is better than in PLA due to their crystalline structure, which may cause to more significant treatment effect on amorphous materials.

It should be noted that in the study of the stress-strain behavior of materials such as ABS and PLA, considering the rheological properties of these materials is crucial. As the current manuscript primarily focuses on the mechanical enhancements achieved through UT, readers seeking a more comprehensive exploration of the rheological behavior during additive manufacturing are encouraged to refer to the work by Sanchez, Beatrice, Lotti, Marini, Bettini, and Costa [19].

The ultimate tensile strength (UTS) of ABS and PLA samples (see Table 4) were extracted from the tensile test diagrams. These data have been analyzed, and surface plots along with the main and interactions plots have been derived. The surface plots of the UTS for ABS and PLA are depicted in Fig. 9. As can be observed in this figure, by decreasing the number of layers from 20 to 10 (i.e., an increase of layer

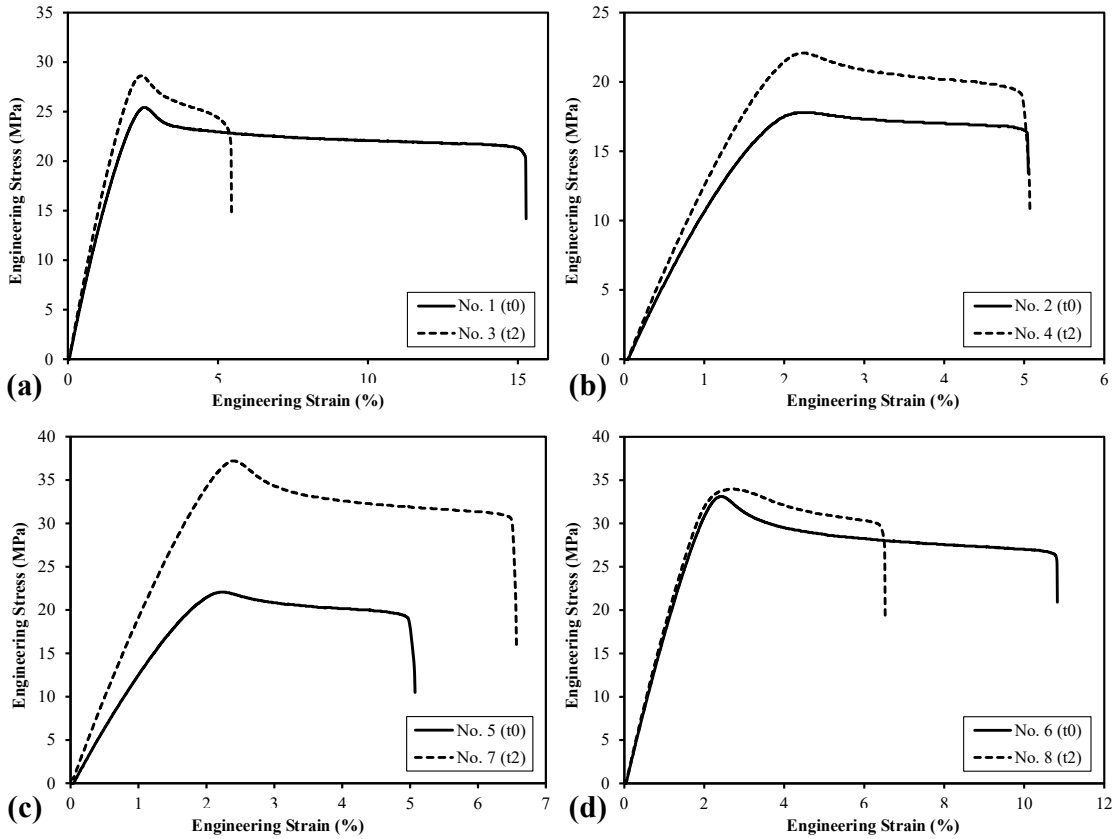

Fig. 8. Comparison of engineering stress-strain curves for PLA samples before and after UT; (a) 60% infill, 10 layers, (b) 60% infill, 20 layers, (c) 100% infill, 10 layers, (d) 100% infill, 20 layers

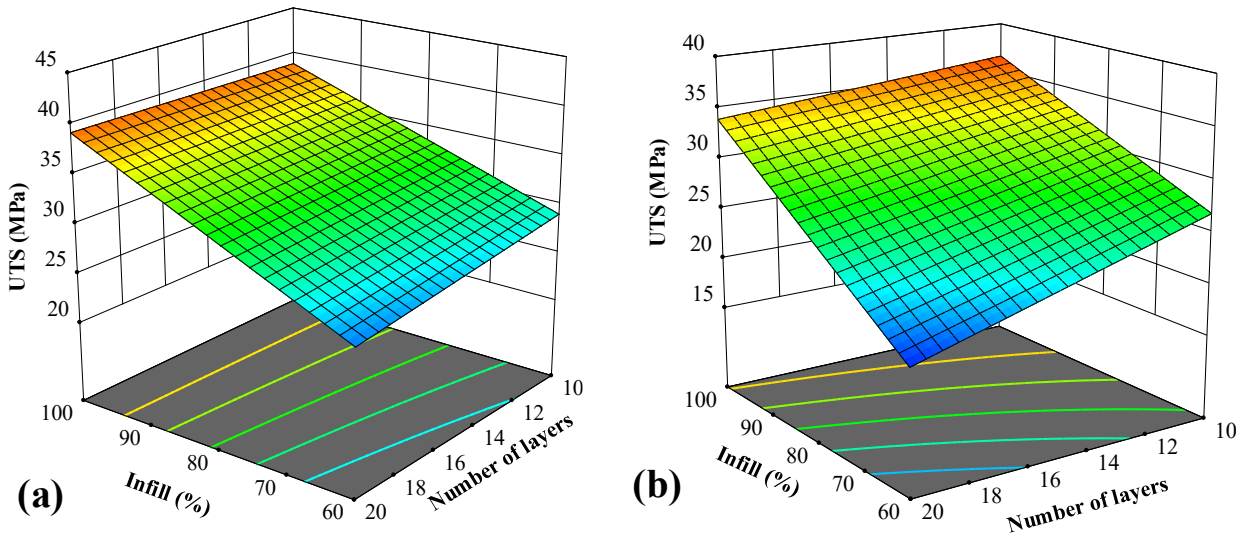

Fig. 9. Surface plot of the effect of the infill percentage and the number of layers on the ultimate tensile strength of (a) ABS and (b) PLA

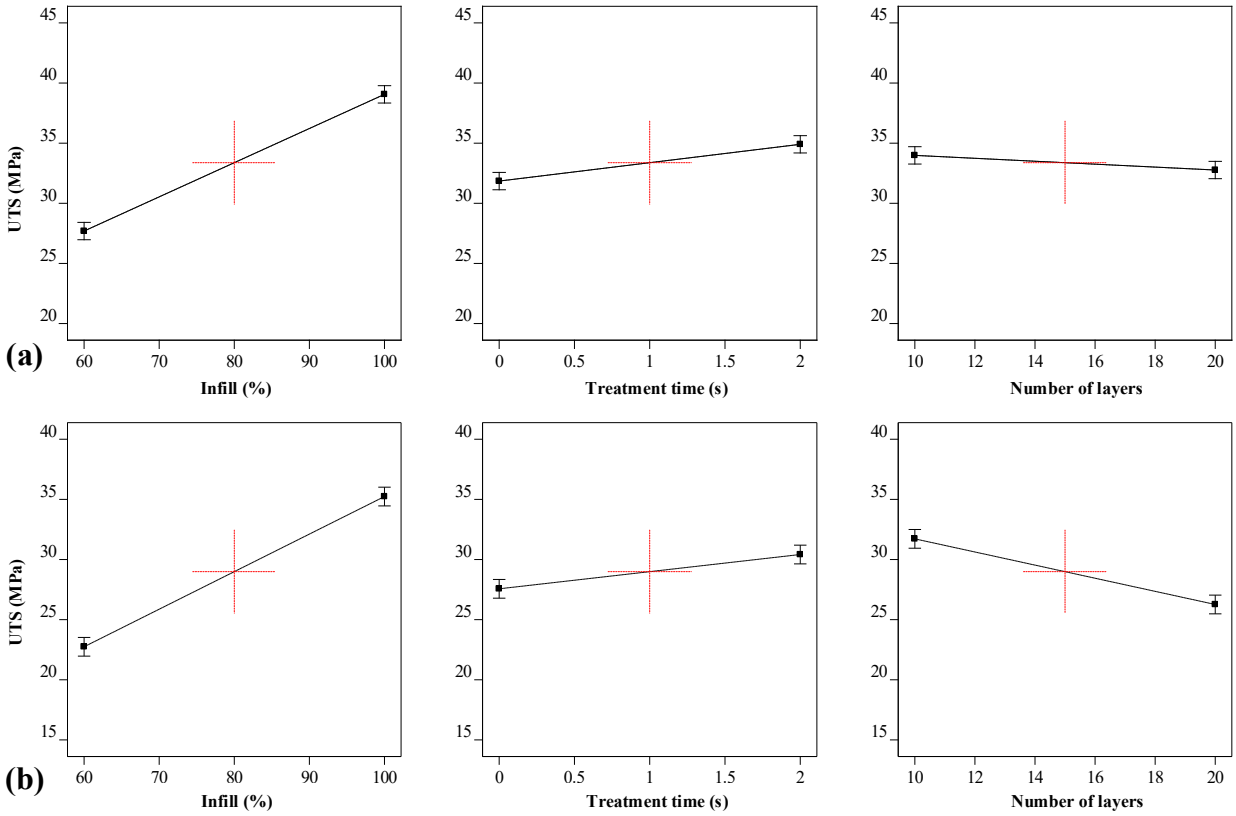

Fig. 10. Main effects plots for tensile strength of (a) ABS and (b) PLA

thickness from 0.15 mm to 0.3 mm), the UTS is increased. Although there are differences in the value of UTS and the curvature of the surface plots in Fig. 9, both ABS and PLA follow a similar trend. The ultrasonically treated samples exhibited the highest UTS, measuring 40.81±0.49 MPa for ABS and 37.94±2.35 MPa for PLA samples.

The main effect and interaction of the studied parameters are illustrated in Figs. 10 and 11. As shown in Fig. 10, the changes in UTS concerning changes in the studied parameters for both ABS and PLA are similar. As the difference between the two levels of infill percentage is quite high, this parameter had the most significant effect on the UTS. Of course, the samples with 100% infill have the highest UTS. After treatment, the bonding of layers increased, and hence the UTS improved. The UTS of ABS and PLA has decreased as the number of layers increases. This observation is in agreement with [20]; however, there is literature (e.g., [21, 22]) that reported the opposite findings. The higher UTS of samples with a lower number of layers could be attributed to the lower number of discontinuities in these samples.

The only noticeable interaction is between the infill percentage and the number of layers, which is illustrated in Fig. 11. This interaction is because the sample is almost solid when the infill percentage is 100. Thus, the UTS is less affected by the change in the number of layers. However, at a lower infill percentage (i.e., 60%), the hollow spaces and discontinuities are highly affected by the number of layers.

3- 2- Fractography

To better understand the changes in the tensile behavior of the ABS and PLA samples, scanning electron microscopy (SEM) images were taken from the fractured sections of the treated and untreated samples. Fig. 12 shows the SEM images from the fracture section of samples ABS #2 and ABS #4. These ABS samples have an infill percentage of 60 and some layers of 20. One may notice that the treated sample (ABS #4) has a lower thickness than the untreated sample (ABS #2). This observation is because the samples have a low infill percentage (60%); thus, the pressure of the ultrasonic horn results in compression and, consequently, thickness reduction. Additionally, in the treated sample, material accumulation is evident, particularly in the top, bottom, and shell layers. The accumulation is a result of partial melting induced by the ultrasonic treatment. It is suspected that the interior gaps have been converted into tiny pores inside the material. This speculation is supported by the fact that such porosities are absent in the untreated sample. The effect of ultrasonic treatment on enhancing bonding between layers and reducing defects has been reported in various investigations [6, 7, 10]. The SEM analysis indicates that both ABS #2 and ABS #4 samples exhibit cleavage planes, suggesting a brittle fracture mechanism [23].

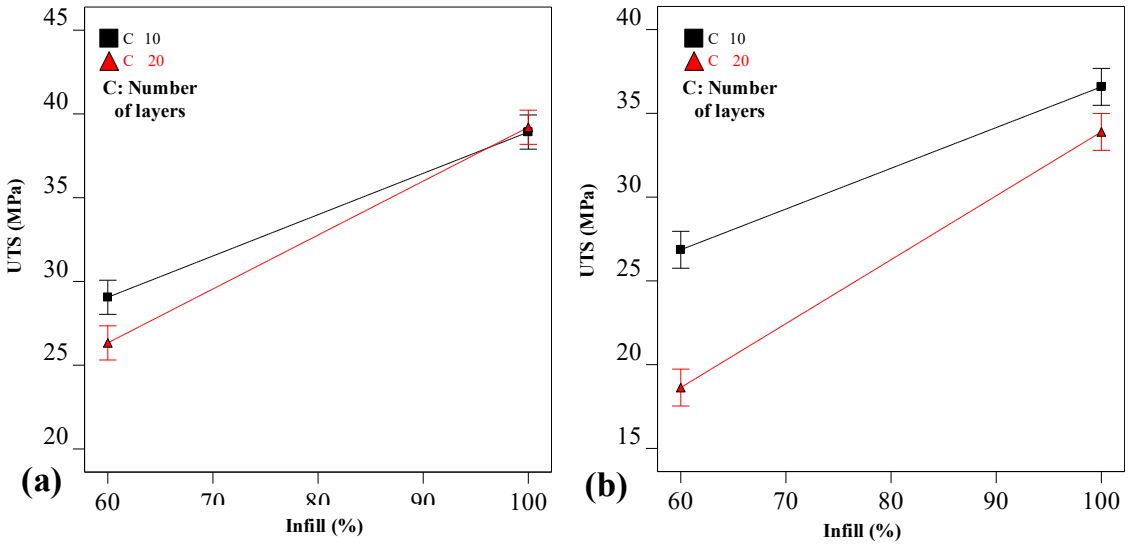

Fig. 11. Interaction of infill percentage and number of layers in predicting ultimate tensile strength for (a) ABS and (b) PLA

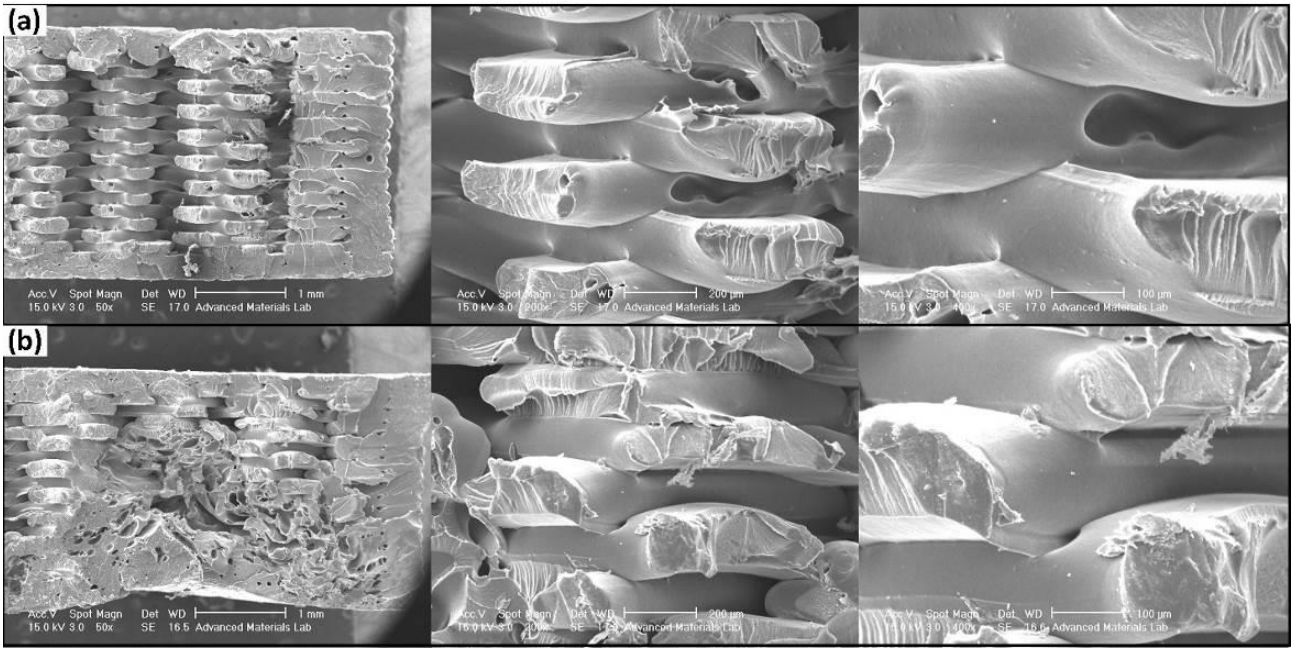

Fig. 12. SEM images from the fracture sections of ABS tensile samples with the infill percentage of 60 (a) #2, without UT, and (b) #4, with UT

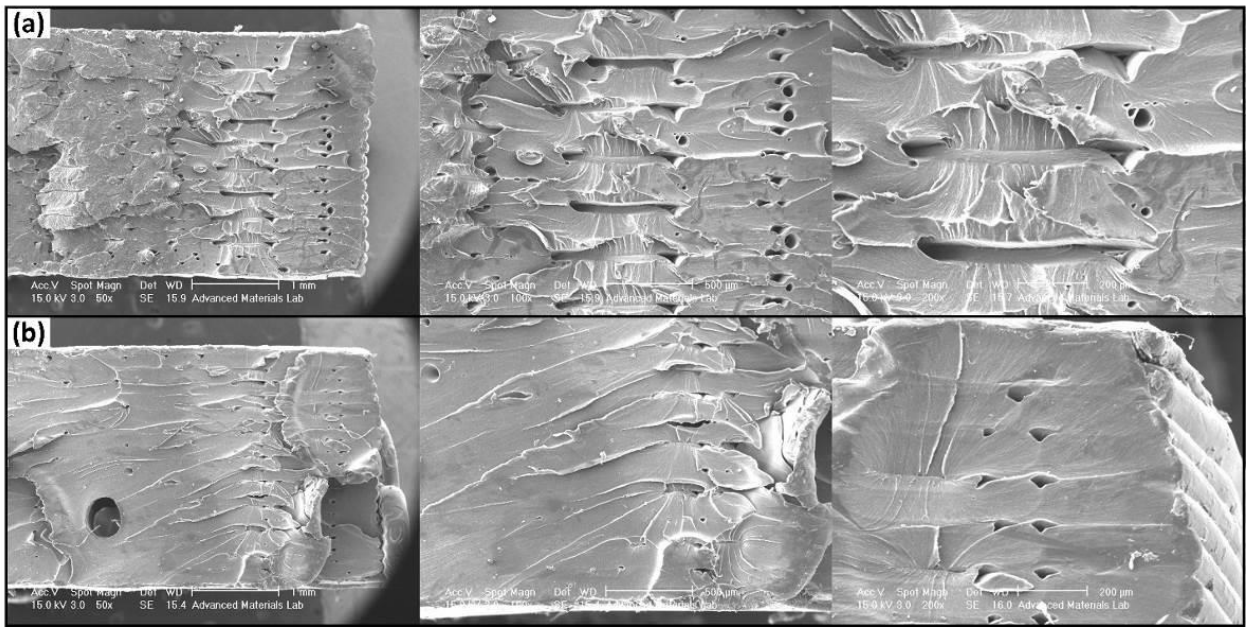

Fig. 13. SEM images from the fracture sections of ABS tensile samples with the infill percentage of 100 (a) #6, without UT, and (b) #8, with UT

In Fig. 13, SEM images depict the fracture sections of ABS tensile samples with 100% infill, comparing the untreated sample (ABS #6) and the ultrasonically treated sample (ABS #8). The untreated sample (Fig. 13a) exhibits a fracture section with visible porosities, indicating the inherent voids and gaps typical of 3D-printed ABS parts. The layers are discernible, and the fracture surface has a somewhat rough appearance. In contrast, the ultrasonically treated sample (Fig. 13b) shows a different morphology. The layers appear more compact, and the porosities are significantly reduced, suggesting that UT has contributed to the fusion of adjacent layers and the reduction of internal voids. The changes observed in Fig. 13 are consistent with the literature on ultrasonic treatment in 3D printing. Ultrasonic vibrations have been reported to induce localized heating in the interlayer regions of 3D-printed samples, promoting partial melting of the polymer material. This melted material tends to flow and fuse, reducing voids and porosities in the structure [10]. The compaction of materials and reduction of porosities are key factors contributing to the enhancement of tensile strength observed in ultrasonically treated samples [6, 10].

SEM images of the fracture sections of PLA tensile samples with an infill percentage of 60 are compared in Fig. 14. The changes in the structure of the PLA samples after UT are comparable to the ones discussed for ABS #2 and ABS #4 (see Fig. 12). The main changes include the reduction of the sample's thickness, the creation of a mass of polymer, and the evolution of small pores due to the trap of empty interior spaces in the structure of the 3D-printed sample. The compaction of materials, especially in the top, bottom, and shell layers, is the reason for the enhancement in the tensile strength of the UTed PLA samples to the untreated samples. Although some regions in PLA #2 have signs of ductile fracture, the cleavage facets imply that the fracture is brittle. On the other hand, the UTed sample (PLA #4) is covered by cleavage facets, and its fracture is brittle. Ultrasonic vibration causes to melting of PLA in some regions, and due to fast cooling at the hold time of vibration, it is possible to change its microstructure from semi-crystalline to amorphous. The brittle fracture facet could be attributed to this reason.

Fig. 15 presents SEM images from the fracture sections of PLA tensile samples with an infill percentage of 100, comparing untreated sample PLA #6 with treated sample PLA #8 after ultrasonic treatment. Analogous to ABS (see Fig. 13), the layers of PLA samples are combined, and the porosity of the section is decreased. According to Fig. 15(a), PLA #6 has many tiny pores before UT, which are distributed in the sample section. However, UT resulted in the reduction and merging of the pores. Furthermore, although there are myriad cleavage facets on the fracture section of the untreated sample, it has a rough appearance. This observation implies that the material experienced some ductile fracture despite the dominant brittle fracture. Thus, it can be concluded that the fracture regime combines ductile and brittle fractures. However, UTed PLA has bigger cleavage facets, and there is no sign of ductile fracture. On the other hand, the dominant fracture regime is a brittle fracture. This change in fracture behavior explains why PLA #8 has much lower elongation in comparison with PLA #6 (see Fig. 8). Overall, the SEM images in Figs. 12 to

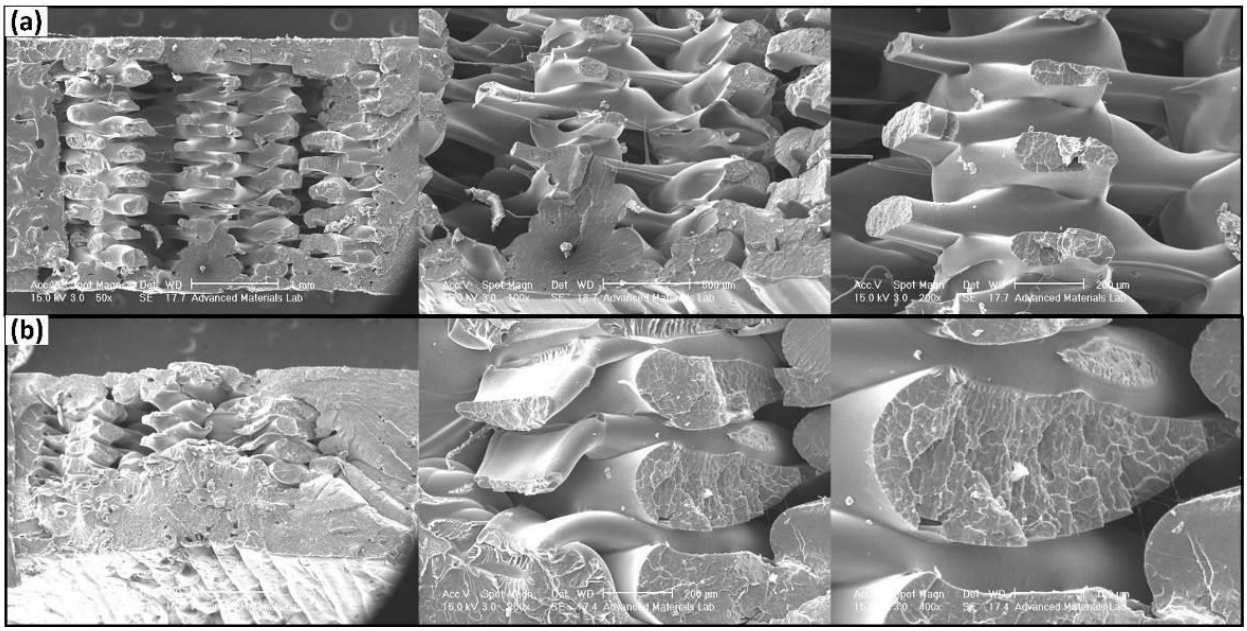

Fig. 14. SEM images from the fracture sections of PLA tensile samples with an infill percentage of 60 (a) #2, without UT, and (b) #4, with UT

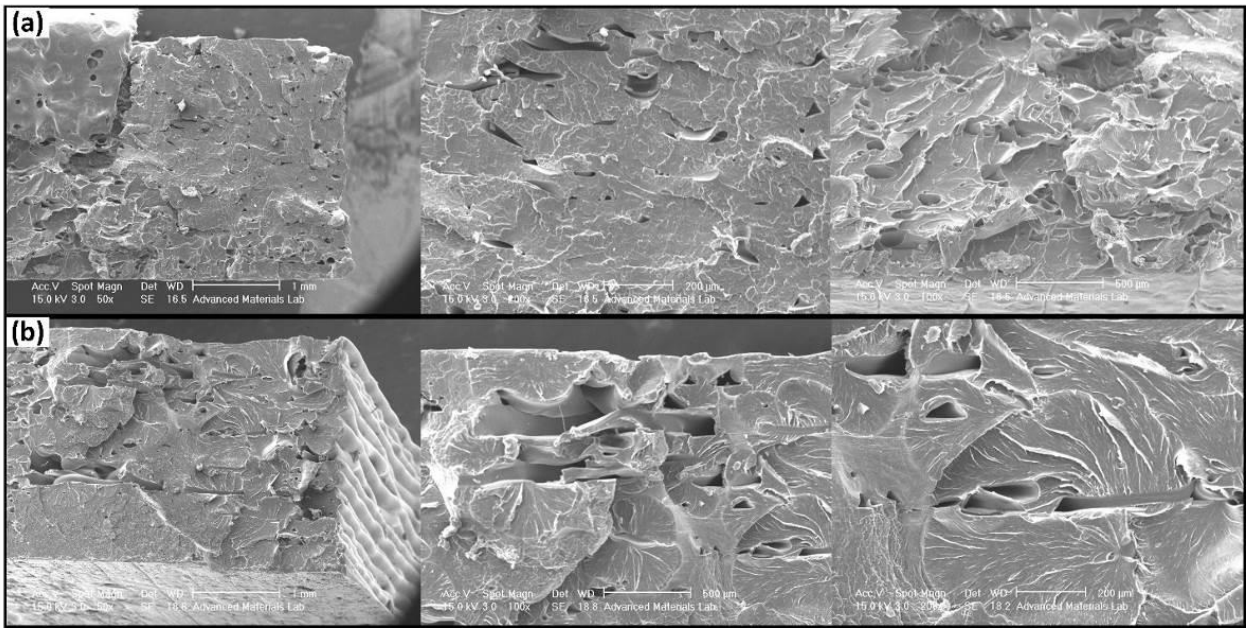

Fig. 15. SEM images from the fracture sections of PLA tensile samples with an infill percentage of 100 (a) #6, without UT, and (b) #8, with UT

15 provide a detailed visual representation of the structural changes induced by UT, supporting the conclusions drawn from the tensile test results and emphasizing the potential of UT as a postprocessing technique for enhancing the mechanical properties of 3D-printed PLA components.

4- Conclusions

This article used ultrasonic vibrations for postprocessing of 3D-printed ABS and PLA samples. The tensile characteristics of the ultrasonic-treated and untreated materials were evaluated. Furthermore, SEM analyses were conducted to determine the effects of the UT on the structure and fracture of the 3D-printed samples. The results can be summarized as follows:

Ultrasonic treatment demonstrated a substantial increase in tensile strength for both ABS and PLA 3D-printed specimens, with an average improvement of 10%. The highest tensile strength was measured at approximately 41 MPa for ABS and 38 MPa for PLA. However, the formability of the materials decreased, and they became more brittle.

The findings indicate that when a larger infill percentage and fewer layers are used, ultrasonic treatment of ABS and PLA samples results in a higher tensile strength. In this study, specimens treated for 2 seconds showed enhanced strength with 100% infill and 10 layers.

The SEM analysis revealed that UT is a promising way to reduce internal porosities naturally developed in 3D printing processes. By setting appropriate values for 3D printing and UT parameters, it is possible to obtain components with lower defects and higher strength.

While the study successfully demonstrated the positive impact of UT on mechanical properties, further investigations are warranted to optimize treatment parameters, such as duration and intensity, to achieve an optimal balance between strength and ductility. The overall quality and performance of the final polymer piece are crucial economic factors. If the hybrid approach results in improved mechanical properties or enhanced product durability, it could justify potential higher costs. This insight contributes to the ongoing discourse on the economic viability of adopting such hybrid approaches in polymer 3D printing.

References

[1] D. Fico, D. Rizzo, R. Casciaro, C. Esposito Corcione, A Review of Polymer-Based Materials for Fused Filament Fabrication (FFF): Focus on Sustainability and Recycled Materials, Polymers, 14(3) (2022) 465.

[2] S. Singh, G. Singh, C. Prakash, S. Ramakrishna, Current status and future directions of fused filament fabrication, Journal of Manufacturing Processes, 55 (2020) 288-306.

[3] A. Safari Mazaheri, V. Abedini, A. Kami, Effects of raster angle and composition of layers on tensile and flexural properties of PLA-PLA/Al multimaterial manufactured by fused deposition modeling, J Proceedings of the Institution of Mechanical Engineers, Part E: Journal of Process Mechanical Engineering, (2023) 09544089231175202.

[4] J.R.C. Dizon, A.H. Espera, Q. Chen, R.C. Advincula, Mechanical characterization of 3D-printed polymers, Additive Manufacturing, 20 (2018) 44-67.

[5] F. Safari, A. Kami, V. Abedini, 3D printing of Continuous Fiber Reinforced Composites: A Review of the Processing, Pre- and Post-Processing Effects on Mechanical Properties, Polym. Polym. Compos., 30 (2022) 1-26.

[6] G. Li, J. Zhao, J. Jiang, H. Jiang, W. Wu, M. Tang, Ultrasonic strengthening improves tensile mechanical performance of fused deposition modeling 3D printing, The International Journal of Advanced Manufacturing Technology, 96(5) (2018) 2747-2755.

[7] W. Wu, J. Li, J. Jiang, Q. Liu, A. Zheng, Z. Zhang, J. Zhao, L. Ren, G. Li, Influence Mechanism of Ultrasonic Vibration Substrate on Strengthening the Mechanical Properties of Fused Deposition Modeling, Polymers, 14(5) (2022) 904.

[8] M. Guivier, J. Kuebler, T. Swanson, C. Lawson, L. Fernandez-Ballester, M. Negahban, M.P. Sealy, Mechanical Behavior of ABS after Interlayer Ultrasonic Peening Printed by Fused Filament Fabrication, in: 2021 International Solid Freeform Fabrication Symposium, University of Texas at Austin, 2021.

[9] A. Tofangchi, P. Han, J. Izquierdo, A. Iyengar, K. Hsu, Effect of Ultrasonic Vibration on Interlayer Adhesion in Fused Filament Fabrication 3D Printed ABS, Polymers, 11(2) (2019) 315-315.

[10] G. Li, J. Zhao, W. Wu, J. Jiang, B. Wang, H. Jiang, J.Y.H. Fuh, Effect of Ultrasonic Vibration on Mechanical Properties of 3D Printing Non-Crystalline and Semi-Crystalline Polymers, Materials, 11(5) (2018) 826-826.

[11] S. Maidin, M. Muhamad, E. Pei, Experimental setup for ultrasonic-assisted desktop fused deposition modeling system, Applied Mechanics and Materials, 761 (2015) 324-328.

[12] K.M.M. Billah, J.L. Coronel, L. Chavez, Y. Lin, D. Espalin, Additive manufacturing of multimaterial and multifunctional structures via ultrasonic embedding of continuous carbon fiber, Composites Part C: Open Access, 5 (2021) 100149.

[13] J. Qiao, Y. Li, L. Li, Ultrasound-assisted 3D printing of continuous fiber-reinforced thermoplastic (FRTP) composites, Additive Manufacturing, 30 (2019) 100926.

[14] A. Bagheri, M.S. Aghareb Parast, A. Kami, M. Azadi, V. Asghari, Fatigue testing on rotary friction-welded joints between solid ABS and 3D-printed PLA and ABS, European Journal of Mechanics - A/Solids, 96 (2022) 104713.

[15] L.C. Paganin, G.F. Barbosa, A comparative experimental study of additive manufacturing feasibility faced to injection molding process for polymeric parts, The International Journal of Advanced Manufacturing Technology, 109(9) (2020) 2663-2677.

[16] Guangzhou Yousu Plastic Technology Co., in, 2023.

[17] . Yang, L. Yang, Digest Ultrasonic Welding I: Localized Heating and Fuse Bonding, arXiv preprint, (2023).

[18] Z. Zhang, X. Wang, Y. Luo, Z. Zhang, L.J.J.o.T.C.M. Wang, Study on heating process of ultrasonic welding for thermoplastics, 23(5) (2010) 647-664.

[19] L.C. Sanchez, C.A.G. Beatrice, C. Lotti, J. Marini, S.H.P. Bettini, L.C.J.T.I.J.o.A.M.T. Costa, Rheological approach for an additive manufacturing printer based on material extrusion, 105 (2019) 2403-2414.

[20] A.a. Alafaghani, A. Qattawi, B. Alrawi, A. Guzman, Experimental Optimization of Fused Deposition Modelling Processing Parameters: A Design-for-Manufacturing Approach, Procedia Manufacturing, 10 (2017) 791-803.

[21] D. Syrlybayev, B. Zharylkassyn, A. Seisekulova, M. Akhmetov, A. Perveen, D. Talamona, Optimisation of Strength Properties of FDM Printed Parts—A Critical Review, Polymers, 13(10) (2021) 1587.

[22] A. Rodríguez-Panes, J. Claver, A.M. Camacho, The Influence of Manufacturing Parameters on the Mechanical Behaviour of PLA and ABS Pieces Manufactured by FDM: A Comparative Analysis, Materials, 11(8) (2018) 1333.

[23] M.S.A. Parast, A. Bagheri, A. Kami, M. Azadi, V. Asghari, Bending fatigue behavior of fused filament fabrication 3D-printed ABS and PLA joints with rotary friction welding, Progress in Additive Manufacturing, 7 (2022) 1345–1361.

HOW TO CITE THIS ARTICLE

V. Fartashvand, A. Kami, A. Bagheri, Enhancing Mechanical Properties of Ultrasonically-Treated 3D-Printed Acrylonitrile-Butadiene-Styrene and Polylactic Acid Parts: A Full Factorial Design Approach, AUT J. Mech Eng., 7(3) (2023) 283-296.

DOI: 10.22060/ajme.2024.22545.6067